ON THE STABILITY OF MANGANESE *TRIS* (β-DIKETONATE) COMPLEXES AS REDOX MEDIATORS IN DSSCs.

Stefano Carli*, Elisabetta Benazzi, Laura Casarin, Tatiana Bernardi, Valerio Bertolasi, Roberto Argazzi, Stefano Caramori, and Carlo Alberto Bignozzi*.

ABSTRACT

The photoelectrochemical properties and stability of DSSCs containing Mn(β-diketonato)$_3$ complexes, [Mn^{III}(acac)$_3$] **1** (acac = acetylacetonate), [Mn^{III}(CF2)$_3$] **2** (CF2 = 4,4-difluoro-1-phenylbutanate-1,3-dione), [Mn^{III}(DBM)$_3$] **3** (DBM = dibenzoylmethanate), [Mn^{II}(CF2)$_3$]TBA (TBA = tetrabutylammonium) **4** and [Mn^{II}(DBM)$_3$]TBA **5**, have been evaluated. At room temperature, the complexes undergo ligand exchange with 4-tert-buthyl-pyridine, an additive commonly used in the solar device to reduce charge recombination at the photoanode. It was also found that the Mn(II)/(III) couple is involved in the dye regeneration process, instead of Mn(III)/(IV) ($E_{1/2}$ > 1V Vs SCE) previously indicated in the literature.

INTRODUCTION

Dye-sensitized solar cells (DSSCs) are essentially biphasic systems in which a mesoporous photoactive substrate (photoanode), usually composed of a wide band gap semiconductor sensitized by appropriate charge-transfer molecules, is in contact with either a liquid or a gel electrolyte containing ionic or molecular species acting as electron mediators which allow for hole transfer to a dark counter electrode.[1]

Since the initial reports,[1,2] most of the research and the industrialization efforts on DSSCs have considered the I_3^-/I^- redox couple as ideal candidate to balance the dual kinetic constraint of fast dye regeneration and slow charge recombination. However, regrettably, this redox couple has a list of undesirable chemical properties: first, the use of iodide based electrolytes results in a large voltage loss across the cell, due to the usually large overpotential for dye regeneration; I_2 in equilibrium with I_3^- is volatile, complicating long term cell sealing; I_3^- is darkly coloured limiting the light harvesting efficiency of the dye; I^-/I_3^- is corrosive and will corrode most metals, posing a serious problem to a long term protection of metallic conductors used to increase the efficiency of electron collection.[3,4] Starting from 2000 the search for alternative electron mediators has become an active field of research,[5,6] exploring the properties of redox tunable transition metal complexes based on Fe(III)/(II),[7,8] Co(III)/(II),[9,10] Ni(IV)/(III)[11] and Cu(II)/(I),[12,13] as well as on organic molecules like TEMPO,[14] and thiolate/disulfide.[15] It was observed that when used in conjunction with specific dye architectures, some of these redox couples allowed to obtain considerably high solar cell efficiencies.[16-18]

Among the first row transition metals, manganese can be considered an interesting candidate for the variety of accessible redox states, its low toxicity and abundance. The first example of application was reported in 2014 by Spiccia et al, which focused on DSSCs containing the commercially available $[Mn(acac)_3]^{0/+1}$ (acac = acetylacetonate) and the MK2 dye, reporting an energy conversion efficiencies of 4.4%, under AM 1.5 G, 100 mW cm^{-2}.[19] Following that report we prepared a series of tris-(β-diketonato) manganese complexes, namely [Mn^{III}(CF2)$_3$] **2** (CF2 = 4,4-difluoro-1-phenylbutanate-1,3-dione), [Mn^{III}(dbm)$_3$] **3** (dbm =

dibenzoylmethanate), [$Mn^{II}(CF2)_3$]TBA **4** and [$Mn^{II}(DBM)_3$]TBA **5** (TBA = tetrabutylammonium), comparing their properties to [$Mn^{III}(acac)_3$] **1**. The study revealed that Mn(II)/(III) is the relevant redox couple involved in the dye regeneration process and that all species are unstable, at room temperature, with respect to ligand exchange with 4-tert-butyl-pyridine (TBP), an additive normally used to reduce charge recombination.[20]

RESULTS AND DISCUSSION

Synthesis

The Mn complexes object of this study are schematized in Figure 1, where **4** and **5** are the reduced form of 2 and 3, respectively.

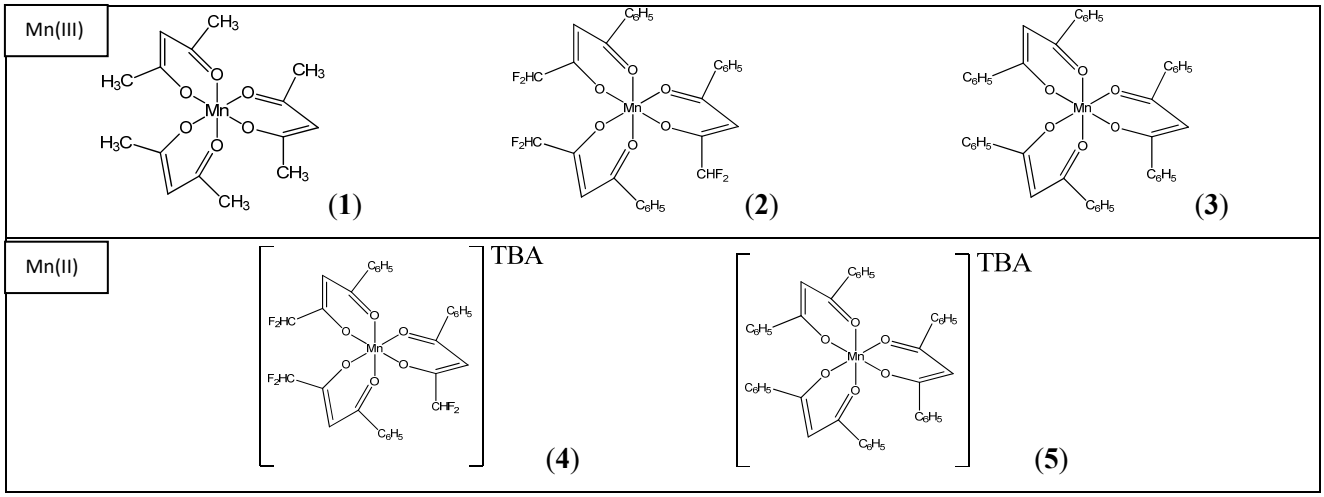

Figure 1. Tris-(β-diketonato) Mn complexes.

Tris-(β-diketonato) Mn(III) complexes are generally prepared by treatment of an aqueous solution of potassium permanganate with acetylacetone.[21-22] . Attempts to prepare **2** and **3,** in high yields, with this method however failed and the two complexes were obtained by treating a solution of Mn(III) acetate with an excess of the respective ligand in hot toluene. The products were then isolated by crystallization in a mixture of diethyl ether and pentane. The divalent manganese complexes **4** and **5** were prepared in high yields by reacting the appropriate ligand with a Mn^{II} precursor in methanol at room temperature. All products were characterized by ESI mass, UV/Vis spectroscopy and cyclic voltammetry. The *fac*-[$Mn(CF2)_3$] **2** complex crystallizes in the trigonal *R-3* space group with the central Mn(III) on the crystallographic special position *3*. Therefore, the complex **2** displays a C_3 symmetry where the three equivalent CF2 ligands exhibit Mn1-O1 and Mn1-O2 distances of 1.978(2) and 1.995(2) Å, respectively (Figure 2, Tables S1a and S1b). Accordingly, the complex which shows a slight distorted octahedral geometry does not display the typical Jahn-Teller distorsion as observed for [$Mn(acac)_3$][22] **1** and [$Mn(DBM)_3$] **3**[23].

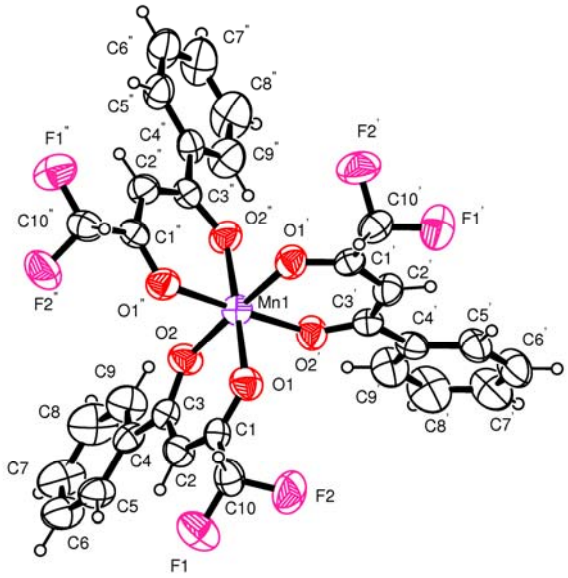

Figure 2. ORTEP drawing of **2**.

ESI mass

Mass characterization of $Mn(acac)_3$ has previously been performed by electron ionization (EI),[24] matrix-assisted laser desorption/ionization time-of-flight mass spectrometry (MALDI-TOFMS),[25] and electrospray ESI[26]. Generally manganese(III) tris(acetylacetonato) exhibits the same dominant fragmentation, namely, the loss of a single ligand yielding the base peak $[Mn(acac)_2]^+$, unlike high pressure EI that can reveal molecular cation radical $[Mn(acac)_3]^{\bullet+}$ (usually of low abundance).[27] The ESI spectra of the commercial $[Mn(acac)_3]$ is reported in Figure S2. As expected, the main peak is relative to $[Mn(acac)_2]^+$ (m/z = 253), but it can be observed a secondary peak at m/z = 294, related to the solvent-complex $[Mn(acac)_2ACN]^+$ (ACN = acetonitrile), the molecular cationic radical $[Mn(acac)_3]^{\bullet+}$ (m/z = 352) and the sodium adduct $[Mn(acac)_3 +Na]^+$ (m/z = 375). A similar fragmentation pattern was observed for **2** and **3** (Figure S3, S4). ESI mass of Mn(II) complexes **4** and **5** were detected in negative ion mode, showing the molecular anions $[Mn(CF2)_3]^-$ and $[Mn(DBM)_3]^-$ as the most intense signals (Figure S5, S6).

Electronic Absorption Spectroscopy.

The electronic absorption spectra of Mn(III) and Mn(II) complexes (Figures S7 and S8), show the typical d-d transitions at wavelengths > 450 nm, with maximum molar extinction coefficients of ca 250 M^{-1} cm^{-1} for Mn (III)[28] and 400 M^{-1} cm^{-1} for Mn(II) species.

Electrochemistry

The electrochemistry of Mn complexes **1**,**2**,**3** has been studied by cyclic voltammetry (CV) in acetonitrile. In Table 1 are reported the relevant electrochemical data. All CVs are characterized by two redox waves corresponding to the oxidation of Mn(III) to Mn(IV), with $E_{1/2}$ in the range of +0.8 ÷ 1.4 V vs SCE, and to the reduction of Mn(III) to Mn(II) in the potential range of $E_{1/2}$, 0 ÷ 0. 5 V vs SCE (Figures S8).[29] The latter process is electrochemically irreversible showing a large peak splitting between reductive and oxidative

processes, most probably consequence of the lack of ligand field stabilization for the high spin d^5 configuration of Mn(II) with consequent large inner sphere contribution to electron transfer, while the former is quasi-reversible.[29]

	$Mn^{II} \rightarrow Mn^{III}$				$Mn^{III} \rightarrow Mn^{IV}$			
	E_{pc} (V)	E_{pa} (V)	ΔE (mV)	$E_{1/2}$ (V)	E_{pc} (V)	E_{pa} (V)	ΔE (mV)	$E_{1/2}$ (V)
$[Mn(acac)_3]$ **1**	-0.37	0.39	760	0.01	0.79	0.97	180	0.88
$[Mn(CF2)_3]$ **2**	0.26	0.64	380	0.45	1.28	1.39	110	1.33
$[Mn(DBM)_3]$**3**	0.00	0.139	139	0.07	0.93	0.99	60	0.96

Table 1. Relevant data obtained from CV analysis of **1**[29-33], **2** and **3**[29] (potentials are referred to SCE).

Photoelectrochemistry

The JV plots of MK2[34] sensitized solar cells, containing $[Mn(acac)_3]$ **1** and $[Mn(CF2)_3]$ **2** as redox mediators, in ACN and MPN are reported in Figure 3. For stability tests, MPN was preferred because of its lower volatility. Complex $[Mn(DBM)_3]$ **3**, was only slightly soluble in MPN, preventing the comparison with the other two mediators at concentration levels of the order of 0.15M. For these reasons MK2 sensitized solar cells were only tested with the redox mediators **1** and **2**.

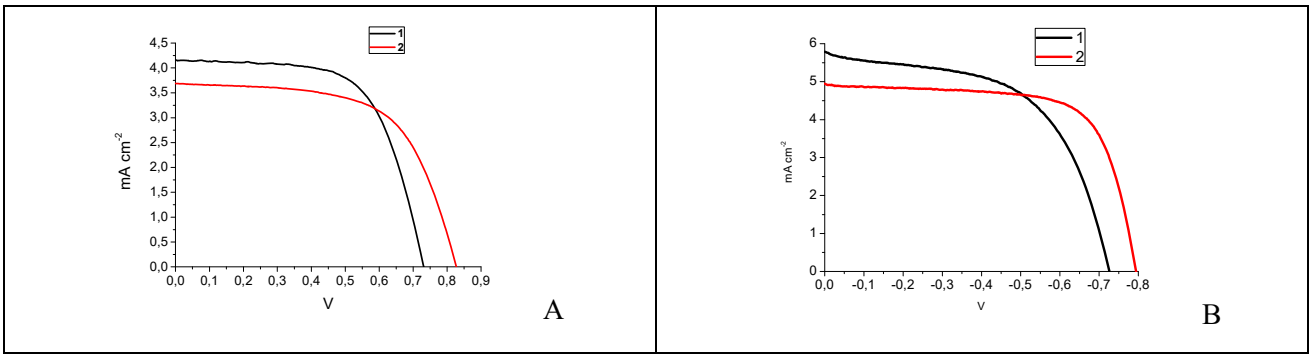

Figure 3. electrolyte composition: 0.15M **1** or **2** , 0.5M TBP, 0.1M $LiCF_3SO_3$, 0.015M $NOBF_4$ in A) MPN and B) ACN.

The higher performances observed in ACN (Figure 3B) are due to the lower solvent viscosity favoring bimolecular electron transfer between oxidized dye and electron mediator. In these experimental conditions, overall efficiencies η%, of the order of 1.6(**1**)÷1.9(**2**), and 2.36(**1**)÷2.72(**2**), were obtained in MPN and ACN respectively. Corresponding short circuit photocurrents, open circuit photovoltages and fill factors are reported in Table S9. For comparison, MK2 sensitized DSSCs were also prepared with an optimized $[Mn(acac)_3]$ acetonitrile based electrolyte, and the results were consistent with previously reported data[19] (see Figure S10 and Table S11).

In general, depending on the dye, both redox couples Mn(II)/(III) and Mn(III)/(IV) can be involved in the regeneration processes. In conjunction with the MK2 dye, Spiccia et[19] al indicated Mn(III) as responsible

for dye regeneration, this contrasts, however, with the thermodynamics of the bimolecular electron transfer process. ΔG values can be obtained from the redox potentials according to: $\Delta G = -ne[(E_{1/2}D^+/D) - (E_{1/2}M^{ox}/M^{red})]$, where *n* is the number of electrons transferred, *e* is the elemental charge of the electron, $E_{1/2}(D^+/D)$ and $E_{1/2}(M^{ox}/M^{red})$ are the redox potentials of the sensitizer and redox mediator, respectively. As reported in the electrochemical section, and supported by literature reports,[29-32] the redox potentials for the couples $[Mn^{III/IV}(acac)_3]^{0/+1}$, $[Mn^{III/IV}(CF2)_3]^{0/+1}$ and $[Mn^{III/IV}(DBM)_3]^{0/+1}$ are +1.12V, +1.57V and +1.20V (Vs NHE) respectively, with the dye exhibiting a reversible $[MK2]^{0/+1}$ process at +1.12V Vs NHE (S12). Considering in addition the redox potential for MK2 adsorbed on TiO_2, which spans from +0.89 V,[35] +0.92 V[19] and +0.96 V[36] Vs NHE, it appears that the Mn(III)/(IV) redox couples cannot be involved in the dye regeneration. From the redox potential (V, vs NHE) of the couples $[Mn^{II/III}(acac)_3]^{-1/0}$ (+0.24), $[Mn^{II/III}(CF2)_3]^{-1/0}$ (+0.69) and $[Mn^{II/III}(DBM)_3]^{-1/0}$ (0.41) driving forces for dye regeneration of 0.88 eV, 0.43 eV and 0.71 eV can be estimated, indicating that Mn(II) is the only species which can effectively reduce the oxidized MK2 dye during cell operation.

Electron Mediator Stability

4-tert-Butylpyridine (TBP) is one of the most useful additives for highly performing DSSC electrolytes, usually allowing for increased cell photovoltage and fill factor. Upon interaction of TBP with the TiO_2 surface, a negative shift of the semiconductor Fermi level and a decreased recombination rate between photoinjected electrons and the oxidized form of the electron mediator (dark current) occur.[37,38] This latter recombination process is important to the point that in the absence of photoanode passivation almost no photocurrent and photovoltage were detected in DSSCs containing Mn(II)/(III) species. At the same time, in steady state irradiation experiments with the reported TBP containing electrolyte composition[19] in either ACN or MPN, we observed a considerable decay of the photoelectrochemical performances. Even in dark conditions at RT, solutions of Mn(II) or of Mn(III) complexes, in the presence of TBP, showed spectral changes indicating modifications of the solution composition, which in the case of **1** was almost complete after 48 h (Figure S13). In neat ACN no appreciable changes of the electronic absorption spectra were observed for **1**, **2, 3,** while for the reduced **4** and **5**, the spectral variations were consistent with oxidation to the corresponding Mn(III) species.

ESI mass spectra revealed that addition of TBP to $[Mn(acac)_3]$ in ACN solution caused an almost immediate appearance of a new peak at m/z = 387 (Figure S14). Except for intensity variations, the ESI profile remained almost unchanged even after 24 hours with the most important peaks relative to the species $[Mn(acac)_2]^+$ m/z = 253, $[Mn(acac)_2ACN]^+$ m/z = 294 and to the species with m/z = 387 which best fit with a $[Mn(acac)_2TBP]^+$ fragmentation adduct. The ability of TBP in coordinating the Mn center was confirmed by X-ray structure on the crystals which spontaneously separated from the solution of ACN of **1** and **2** containing TBP. Figure 4 shows the structure of trans-$[Mn^{III}(acac)_2TBP_2]ClO_4$ and trans-$[Mn^{II}(CF2)_3TBP_2]^0$, where the higher oxidation potential stabilizes Mn(II) in the complex; the corresponding crystallographic data are reported in Tables S15a,b and S16a,b.

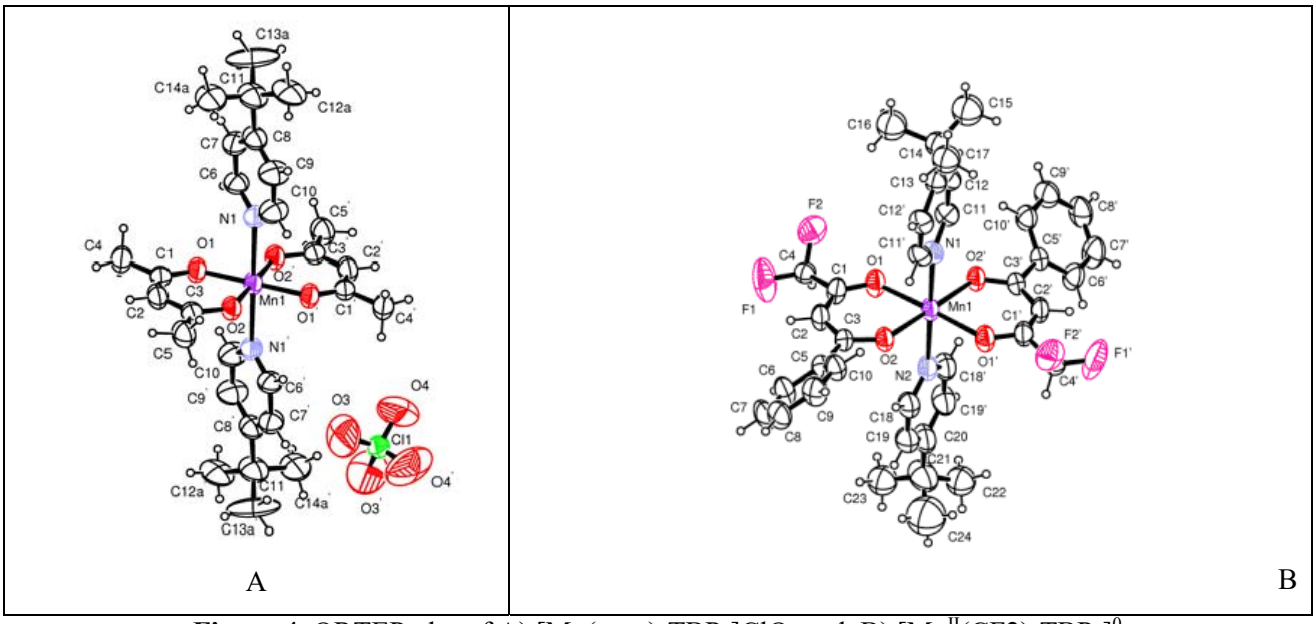

Figure 4. ORTEP plot of A) $[Mn(acac)_2TBP_2]ClO_4$ and B) $[Mn^{II}(CF2)_3TBP_2]^0$.

A similar behavior was observed for compound **3**, but in this case it was not possible to obtain crystals of the TBP containing complex due to its lower solubility in ACN. ESI profile confirms the same decomposition pattern observed for **1** and **2**, with the m/z = 636 which best fit with the $[Mn(DBM)_2TBP]^+$ fragmentation adduct (Figure S17). Attempts to use benzimidazole derivatives led to similar electrolyte instability.

In order to improve electrolyte stability and to suppress at the same the dark current, in the absence of nitrogen based Lewis bases as TiO_2 passivating agents, we performed a series of experiments by using APTS silanized photoanodes[39], sensitized with the Z907 dye, in the presence of the redox mediator **4** and **5** and of the corresponding oxidized forms **2** and **3**. Contrary to MK2, Z 907 was found to exhibit a good adsorption stability following trialkoxysilane post-treatments of the sensitized photoanode[39,40] and was thus the first dye to be considered for these studies. TiO_2 post functionalization with short chain siloxanes[39] were found to successfully screen the semiconductor surface from electron acceptors in the electrolyte by acting mainly through sterical blocking against neutral Mn(III) complexes. Sealed DSSCs showed an appreciable response, despite the absence of basic additives, reaching quickly the steady state under 1 sun and potential cycling at 10 mV/s (Figure 5), corresponding to overall efficiencies of 2.33% and 1.84% for $[Mn^{II/III}(CF2)_3]^{-1/0}$ and $[Mn^{II/III}(DBM)_3]^{-1/0}$ respectively.

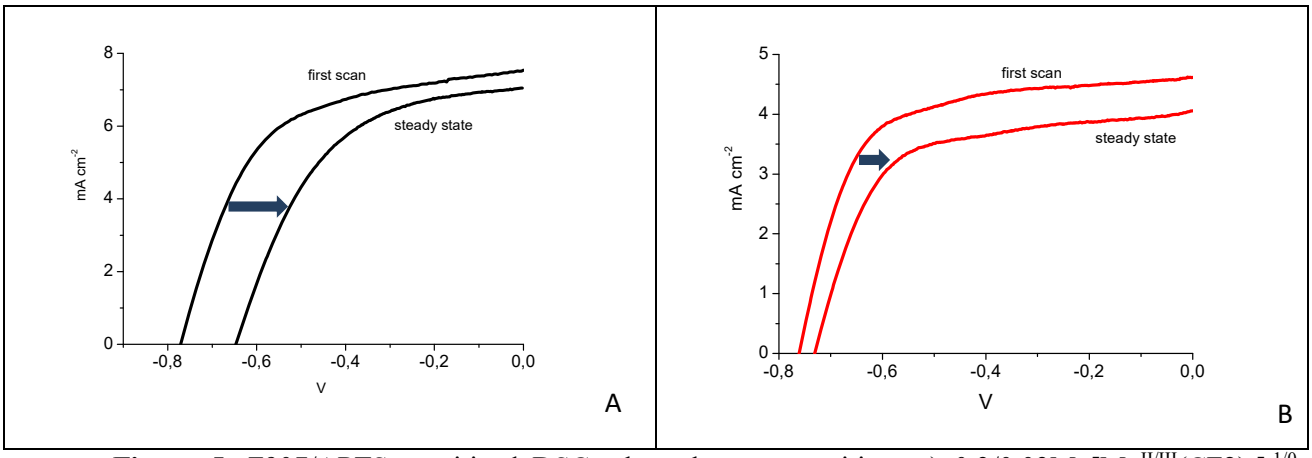

Figure 5. Z907/APTS sensitized DSC, electrolyte composition: a) 0.3/0.03M $[Mn^{II/III}(CF2)_3]^{-1/0}$, 0.1M LiTf, ACN b) 0.3/0.03M $[Mn^{II/III}(DBM)_3]^{-1/0}$ 0.1M LiTf, ACN/DMF 1:1 vol.

We believe that Z907 is not the best dye to be used in conjunction with the investigated electron mediators, most probably more sterically hindered dyes like MK2 with a stronger binding group[41] would result compatible with APTS, or other passivation methods, allowing for better cell performances, and work is in progress in this direction.

CONCLUSIONS

In conclusion we found that the reactivity towards TBP of tris(β-diketonate)Mn complexes, limits their use as redox mediators in DSSCs. Based on the electrochemical characterization, the effective redox couple intercepting both the previously investigated MK2[19] and Z907 (this study) dyes is Mn(II)/(III). To date, the results obtained with Mn are quite unsatisfactory but it can be foreseen that the use of sterically hindered dyes, compatible with an appropriate photoanode passivation may lead to better DSSC performances.

EXPERIMENTAL SECTION

Materials. All chemicals were Sigma Aldrich products and were used as received. Conductive FTO (fluorine tin oxide) TEC8, 2.3 mm thick substrates (Pilkington) were carefully cleaned by several washings in ethanol, acetone, and Alconox followed by annealing at 400 °C in air before use. TiO_2 colloidal paste (DSC 18NRT) was purchased from Dyesol. Mass spectrometry was performed in ESI mode with a Finningan LCQDuo Ion Trap (Capillary Temp: 250 °C, Infusion flow rate: 18 µL/min, Sheath gas flow rate: 20 AU), or with a Waters Micromass ZQ 2000 (Cone Temperature 110°C and desolvation Temperature of 130°C, Capillary voltage 2.30 KV, Cone Voltage 20 V, Extractor Voltage 3V and RF Lens Voltage 0.3V, Flow rate 295 L/hr) under positive/negative mode acquisition. Cyclic Voltammetry plots were collected in a standard three-electrode cell with an Autolab PGSTAT 302/N potentiostat at a scan rate of 100 mV s^{-1} with a standard calomel electrode as reference, a Pt wire as auxiliary, and a glassy carbon as working electrode. Absorption spectra were collected with a JASCO V 570 UV–Vis spectrophotometer.

Synthesis of Mn(III) complexes. A stirred solution of $Mn(CH_3COO)_3 \times 2H_2O$ (200 mg, 0.74 mmol) in toluene (25 mL) was treated with an excess of the ligand (CF2 or DBM) (4.93 mmol). The mixture was heated under stirring for 6 hours, cooled to room temperature and the solvent was removed with a rotavapor. The residue was dissolved in the minimum amount of diethyl ether and n-exane was added until a green to brown solid separated. After several hours the precipitate was filtrated under vacuum and washed several times with n-exane. Yields in the range of 50÷60%. **[Mn(CF2)$_3$] (2).** m/z (ESI): 449 $[Mn(CF2)_2]^+$ calculated for $C_{30}H_{21}F_6MnO_6$ 646.2. ε_{560} (M cm^{-1}): 216. **[Mn(DBM)$_3$] (3).** m/z (ESI): 501 $[Mn(DBM)_2]^+$ calculated for $C_{45}H_{33}MnO_6$ 724.2. ε_{560} (M cm^{-1}): 170.

Synthesis of [Mn(CF2)$_3$]TBA (4). A stirred solution of $Mn(CH_3COO)_2 \times 4H_2O$ (1 mmol) in methanol (25 mL) and TBAPF6 (1 mmol) was treated, at room temperature, with a solution of CF2 (3 mmol) in the minimum amount of methanol. The yellowe/orange solid was separated by filtration under vacuum and washed several times with cold methanol. Yields in the order of 50%. m/z (ESI): 646 $[Mn(CF2)_3]^-$ calculated for $C_{30}H_{21}F_6MnO_6$ 646.2. ε_{450} (M cm^{-1}): 370.

Synthesis of [Mn(DBM)$_3$]TBA (5). DBM (3 mmol) was added to a stirred solution of TBAOH (3 mmol, 30% mol in methanol) in methanol (25 mL). The stirred solution was treated, at room temperature, with a $MnCl_2 \times 6H_2O$ (1 mmol) dissolved in the minimum amount of methanol. The yellowe/orange solid was separated by filtration under vacuum and washed several times with cold methanol. Yields were of the order of 60%. m/z (ESI): 724 $[Mn(DBM)_3]^-$ calculated for $C_{45}H_{33}MnO_6$ 724.2. ε_{450} (M cm^{-1}): 273.

Solar Cell Fabrication. Mesoporous titania films (ca. 6 μm thick) were prepared by blading a commercial colloidal TiO_2 paste on FTO electrodes, which were left to dry under a gentle warm air stream before sintering at 450 °C for 30 min. The resulting transparent films were immersed in a 0.4 M $TiCl_4$ solution for 12 hours, rinsed with water and gradually heated at 500°C for 10 minutes. Finally, the photoanodes were immersed in a 0.2 mM solution of MK2 in a 1:1 toluene/acetonitrile mixture for 24 h. Solar cells were assembled by holding the two electrodes together with metallic clamps and by using a 25 μm thick Surlyn frame as spacer. PEDOT based counter electrodes was prepared by potentiostatic anodic electropolymerization of 3,4-ethylenedioxythiophene (EDOT) on FTO glasses.[42]

Electrolyte Formulation. The electrolyte composition consisted of 0.15M **1** or **2**, 0.5M TBP, 0.1M $LiCF_3SO_3$, 0.015M $NOBF_4$ in a) MPN and b) ACN for JV shown in Figure 3, and a) $[Mn^{II/III}(CF2)_3]^{-1/0}$ 0.3/0.03M, 0.1M $LiCF_3SO_3$, ACN b) $[Mn^{II/III}(DBM)_3]^{-1/0}$ 0.1M LiTf, ACN/DMF 1:1 vol. for JV shown in Figure 5.

Solar Cell Characterization. Current−voltage measurements were performed with an Autolab PGSTAT 302/N potentiostat at a scan rate of 20 mV s^{-1}. Cell performances were evaluated under AM 1.5 illumination (ABET sun simulator).

Stability test. A 0.15M $[Mn(acac)_3]$ or $[Mn(dpfb)_3]$ in 0.1 M $LiClO_4$ was treated with 0.5M TBP in acetonitrile. The solution was kept under dark at room temperature. For the UV/Vis test a fixed amount of this solution was diluted with acetonitrile to a final concentration of 1.2×10^{-4} M.

Crystallization of complexes. Dark-green crystals of **2** were obtained by slow evaporation of the solvent from a 0.15M solution in ACN. Yellow/orange crystals spontaneously separated by the electrolyte solution after two weeks or 24 hours for *trans*-$[Mn^{III}(acac)_2TBP_2]ClO_4$ and *trans*-$[Mn^{II}(CF2)_3TBP_2]^0$ respectively.

Crystallography. The crystal data of compounds *fac*-$[Mn(CF2)_3]$ **2**, *trans*-$[Mn^{III}(acac)_2TBP_2]ClO_4$ and *trans*-$[Mn^{II}(CF2)_3TBP_2]^0$ were collected at room temperature using a Nonius Kappa CCD diffractometer with graphite monochromated Mo-Kα radiation. The data sets were integrated with the Denzo-SMN package[43] and corrected for Lorentz, polarization and absorption effects (SORTAV)[44]. The structures were solved by direct methods using SIR97[45] system of programs and refined using full-matrix least-squares with all non-hydrogen atoms anisotropically and hydrogens included on calculated positions, riding on their carrier atoms. All calculations were performed using SHELXL-97[46] and PARST[47] implemented in WINGX[48] system of programs. The Figures have been drawn using the program ORTEP[49]. The crystal data are given in the Supporting Material.

Crystallographic data have been deposited at the Cambridge Crystallographic Data Centre and allocated the deposition numbers CCDC1421029-1421030-1421031. These data can be obtained free of charge via www.ccdc.cam.ac.uk/conts/retrieving.html or on application to CCDC, Union Road, Cambridge, CB2 1EZ, UK [fax: (+44)1223-336033, e-mail: deposit@ccdc.cam.ac.uk]

NOTES AND REFERENCES

(1) O'Regan, B.; Graetzel, M. *Nature* **1991**, *353*, 737−740.
(2) Hagfeldt, A.; Graetzel, M. *Acc. Chem. Res.* **2000**, *33*, 269.
(3) Nusbaumer, H.; Zakeeruddin, S. M.; Moser, J. E.; Graetzel, M. *Chem. Eur. J.* **2003**, *9*, 3756.
(4) Toivola, M.; Ahlskog, F.; Lund, P. *Sol. Energ. Mat. Sol. Cells* **2006**, *90*, 2881.
(5) Wu, J.; Lan, Z.; Lin, J.; Huang, M.; Huang, Y.; Fan, L.; Luo, G. *Chem. Rev.* **2015**, *115*, 2136−2173.
(6) Bignozzi, C. A.; Argazzi, R.; Boaretto, R.; Busatto, E.; Carli, S.; Ronconi, F.; Caramori, S. *Coord. Chem. Rev.* **2012**, *257*, 1472.
(7) Caramori, S.; Husson, J.; Beley, M.; Bignozzi, C. A.; Argazzi, R.; Gros, P. C. *Chem. Eur. J.* **2010**, *16*, 2611−2618.
(8) Gregg, B. A.; Pichot, F.; Ferrere, S.; Fields, C. L. *J. Phys. Chem. B* **2001**, *105*, 1422.
(9) Sapp, S. A.; Elliott, C. M.; Contado, C.; Caramori, S.; Bignozzi, C. A. *J. Am. Chem. Soc.* **2002**, *124*, 11215−11222.
(10) Nusbaumer, H.; Moser, J. E.; Zakeeruddin , S. M.; Nazeeruddin, M. K.; Graetzel, M. *J. Phys. Chem. B* **2001**, *105*, 10461−10464.
(11) Li, T. C.; Spokoyny, A. M.; She, C.; Farha, O. K.; Mirkin, C. A.; Marks, T. J.; Hupp, T. J. *J. Am. Chem. Soc.* **2010**, *132*, 4580−4582.
(12) Hattori, S. W., Y.; Yanagida, S.; Fukuzumi, S. *J. Am. Chem. Soc.* **2005**, *127*, 9648−9654.
(13) Bai, Y.; Yu, Q.; Cai, N.; Wang, Y.; Zhang, M.; Wang, P. *Chem. Commun.* **2011**, *47*, 4376−4378.
(14) Zhang, Z.; Chen, P.; Murakami, T. N.; Zakeeruddin, S. M.; Graetzel, M. *Adv. Funct. Mater.* **2008**, *18*, 341−346.
(15) Wang, M.; Chamberland, N.; Breau, L.; Moser, J. E.; Humphry-Baker, R.; Marsan, B.; Zakeeruddin, S. M.; Graetzel, M. *Nat. Chem.* **2010**, *2*, 385−389.

(16) Feldt, S. M.; Gibson, E. A.; Gabrielsson, E.; Sun, L.; Boschloo, G.; Hagfeldt, A. *J. Am. Chem. Soc.* **2010**, *132*, 16714−16724.

(17) Daeneke, T.; Kwon, T. H.; Holmes, A. B.; Duffy, N. W.; Bach, U.; Spiccia, L. *Nat. Chem.* **2011**, *3*, 211−215.

(18) Tsao , H. N.; Yi , C.; Moehl, T.; Yum, J. H.; Zakeeruddin, S. M.; Nazeeruddin, M. K.; Graetzel, M. *ChemSusChem* **2011**, *4*, 591

(19) Perera, I. R.; Gupta, A.; Xiang, W.; Daeneke, T.; Bach, U.; Evans, R. A.; Ohlin, C. A.; Spiccia, L. *Phys. Chem. Chem. Phys.* **2014**, *16*, 12021.

(20) Nazeeruddin, M. K.; Kay, A.; Rodicio, I.; Humpbry-Baker, R.; Miiller, E.; Liska, P.; Vlachopoulos, N.; Gratzel, M. *J. Am. Chem. Soc.* **1993**, *115*, 6382.

(21) Bhattacharjee, M. N.; Chaudhuri, M. K.; Khathing, D. T. *Journal of the Chemical Society, Dalton Transactions* **1982**, 669.

(22) Geremia, S.; Demitri, N. *J. Chem. Educ.* **2005**, *82* 460.

(23) Freitag, R.; Muller, T. J.; Conradie, J. *J. Chem. Crystallogr.* **2014**, *45*, 352.

(24) Bancroft, G. M.; Reichert, C.; Westmore, J. B. *Inorg. Chem.* **1968**, *7*, 870.

(25) Wyatt, M. F.; Havard, S.; Stein, B. K.; Brenton, A. G. *Rapid Commun. Mass Spectrom.* **2008**, *22*, 11.

(26) Henderson W., M. J. S. *Mass Spectrometry of Inorganic and Organometallic Compounds: Tools - Techniques – Tips*; John Wiley & Sons, 2005.

(27) Schildcrout, S. M. *J. Phys. Chem.* **1976**, *80*, 2834.

(28) Barnum, D. W. *J. Inorg. Nucl. Chem.* **1961**, *21*, 221.

(29) Freitag, R.; Conradie, J. *Electrochim. Acta* **2015**, *158* 418.

(30) Pacześniak, T.; Błoniarz, P.; Rydel, K.; Sobkowiak, A. *Electroanalysis* **2007** *9*, 945.

(31) Bond, A. M.; Martin, R. I.; Master, s. A. F. *Inorg. Chem.* **1975** *14*, 1432.

(32) Richert, S. A.; Tsang, P. K. S.; Sawyer, D. T. *Inorg. Chem.* **1989** *28* 2471.

(33) Gritzner, G.; Murauer, H.; Gutmann, V. *J. Electroanal. Chem.* **1979**, *101*, 185.

(34) Koumura, N.; Wang, Z. S.; Mori, S.; Miyashita, M.; Suzuki, E.; Hara, K. *J. Am. Chem. Soc.* **2006**, *128*, 14256.

(35) Daeneke, T.; Mozer, A. J.; Uemura, Y.; Makuta, S.; Fekete, M.; Tachibana, Y.; Koumura, N.; Bach, U.; Spiccia, L. *J. Am. Chem. Soc.* **2012**, *134*, 16925.

(36) Wang Z. S., K. N., Cui Y., Takahashi M., Sekiguchi H., Mori A., Kubo T., Furube A., Kohjiro H. *Chem. Mater.* **2008**, *20*, 3993.

(37) Nazeeruddin M. K., K. A., Rodicio I., Humpbry-Baker R., Miiller E., Liska P., Vlachopoulos N., Gratzel M. *J. Am. Chem. Soc.* **1993**, *115*, 6382.

(38) Koh, T. M.; Nonomura, K.; Mathews, N.; Hagfeldt, A.; Grätzel, M.; Mhaisalkar, S. G.; Grimsdale, A. C. *J. Phys. Chem. C* **2013**, *117*, 15515−15522.

(39) Carli, S.; Casarin, L.; Caramori, S.; Boaretto, R.; Busatto, E.; Argazzi, R.; Bignozzi, C. A. *Polyhedron* **2014**, *82*, 173.

(40) Mba, M.; D'Acunzo, M.; Salice, P.; Maggini, M.; Caramori, S.; Campana, A.; Aliprandi, A.; Argazzi, R.; Carli, S.; Bignozzi, C. A. *J. Phys. Chem. C* **2013**, *117*, 19885−19896.

(41) Kakiage, K.; Aoyama, Y.; Yano, T.; Otsuka, T.; Kyomen, T.; Unno, M.; Hanaya, M. *Chem. Commun.* **2014**, *50*, 6379.

(42) Carli, S.; Busatto, E.; Caramori, S.; Boaretto, R.; Argazzi, R.; Timpson, C. J.; Bignozzi, C. A. *J. Phys. Chem. C* **2013**, *117*, 5142−5153.

(43) Otwinowski, Z.; Minor, W. *Methods in Enzymology (Macromolecular Crystallography Part A)* **1997**, *276*, 307.

(44) Blessing, R. H. *Acta Crystallogr. Sect A* **1995**, *51*, 33.

(45) Altomare, A. B., M. C.; Camalli,M.; Cascarano, G. L.; Giacovazzo, C.; Guagliardi, A.; Moliterni, A. G.; Polidori G.; Spagna, R. *J. Appl. Crystallogr.* **1999**, *32*, 115.

(46) Sheldrick, G. M. *Program for Crystal Structure Refinement, University of Gottingen, Germany* **1997**.

(47) Nardelli, M. *J. Appl. Crystallogr.* **1995**, *28*, 659.

(48) Farrugia, L. J. *J. Appl. Crystallogr.* **1999**, *32*, 837.

(49) Burnett M. N.; Johnson, C. K. *ORTEP III, Report ORNL-6895, Oak Ridge National Laboratory, Oak Ridge, TN* **1996**.